Research Paper

Journal of Engineering and Technological Sciences

Charring Depth and Charring Rate of Resak and Jelutong Timber Beams in Two-Dimensional Fire

Lannie Francis[1,2], Ahmad Beng Hong Kueh[3,4], Norshariza Mohamad Bhkari[1,5], Zakiah Ahmad[1,*], Hafizah Muhamad Azlan[1,6] & Muhammad Bazli Faliq Mohd Puaad[7]

[1]Faculty of Civil Engineering, Universiti Teknologi MARA, 40450 Shah Alam, Selangor, Malaysia
[2]Faculty of Civil Engineering, Universiti Teknologi MARA, Sarawak Branch, Kota Samarahan Campus, 94300 Kota Samarahan, Sarawak, Malaysia
[3]Department of Civil Engineering, Faculty of Engineering, Universiti Malaysia Sarawak, 94300 Kota Samarahan, Sarawak, Malaysia
[4]UNIMAS Water Centre (UWC), Faculty of Engineering, Universiti Malaysia Sarawak, 94300 Kota Samarahan, Sarawak, Malaysia
[5]Institute for Infrastructure Engineering and Sustainable Management (IIESM), Universiti Teknologi MARA, 40450 Shah Alam, Selangor, Malaysia
[6]Faculty of Civil Engineering, Universiti Teknologi MARA, Penang Branch, Permatang Pauh Campus, 13500 Permatang Pauh, Malaysia
[7]Faculty of Civil Engineering, Universiti Teknologi MARA, Johor Branch, Pasir Gudang Campus, 81750 Masai, Johor Darul Ta'zim, Malaysia

*Corresponding author: zakiah@uitm.edu.my

Abstract

Wood is a widely used material in building construction and infrastructure due to its environmental sustainability and economic benefits. However, timber structures are inherently vulnerable to fire hazards because of the combustible nature of wood. When exposed to fire, the strength and stiffness of timber members significantly decrease as a result of the charring process. In fire design for timber structures, charring depth and charring rate are critical parameters used to evaluate fire performance. This study aimed to investigate the charring characteristics, specifically, the charring depth and rate of solid timber from two Malaysian tropical hardwood species, namely Resak (Cotylelobium sp.), with a density of 1019 kg/m³, and Jelutong (Dyera costulata sp.), with a density of 506 kg/m³. Three beams from each species were subjected to a two-dimensional fire exposure for 60 minutes, following the standard fire testing procedure outlined in BS 476-20. The results indicated that Resak exhibited a lower lateral charring depth compared to Jelutong, averaging 25 mm and 45 mm, respectively. However, the bottom-side charring depths were similar for both species, measuring 54 mm for Resak and 53 mm for Jelutong. In terms of charring rate, Resak showed a lower value of 0.48 mm/min, while Jelutong had a higher rate of 0.83 mm/min. Both values fall within the acceptable range specified in Eurocode 5. A clear understanding of timber charring behavior, including both depth and rate, is essential for the safe and effective design of timber structures under fire conditions.

Keywords: *char depth; density; fire resistance; jelutong timber; resak timber; two-dimensional charring rate.*

Introduction

Timber has been used as a construction material for centuries due to its inherent strength, aesthetic appeal, and environmental sustainability. Despite these advantages, timber is a combustible material, and it is often mistakenly perceived by local building authorities, property owners, contractors, and even designers as having poor fire resistance.

While timber does burn, it behaves in a predictable and, in some ways, beneficial manner under fire conditions. When exposed to fire, timber undergoes thermal degradation and pyrolysis, leading to a loss of mechanical properties such as strength and stiffness. This process produces combustible gases, inorganic ash, and a carbon-rich residue known as char (Richter & Rein, 2019; Friquin, 2011). As illustrated in Figure 1, the charred area (blackened region) forms on the exposed

ISSN: 2337-5779
DOI: 10.5614/j.eng.technol.sci.2026.58.4.8

DOI: 10.5614/j.eng.technol.sci.2026.58.4.8

surfaces of timber elements. The charring line, which demarcates the boundary between the charred and uncharred wood typically coincides with the 300°C isotherm (Richter et al., 2021; Cachim & Franssen, 2009). The charring depth is defined as the distance from the original timber surface to the location of the char line. Although the char layer itself has no structural integrity, it plays a critical role in fire resistance by insulating and protecting the inner, unburned core of the timber. This layer slows down heat penetration, thereby reducing further material degradation, cross-sectional loss, and weight reduction (Li et al., 2015; Peng et al., 2010). Wood's natural insulating behavior is a result of its low thermal conductivity and its tendency to form a protective char layer when exposed to elevated temperatures (around 300°C). The progression of this char layer over time during fire exposure is referred to as the charring rate, a key parameter in fire design for timber structures.

Figure 1 The char layer and unheated timber.

Understanding the charring rate is fundamental in assessing the fire resistance of timber elements, as it directly influences how rapidly the load-bearing cross-sectional area of timber is reduced during fire exposure.

In the context of fire safety design, this rate determines how long a timber member can maintain its structural integrity under elevated temperatures. Therefore, it is essential for structural engineers and designers to incorporate charring rate data into their calculations to ensure that timber components can withstand fire loads not only during the fire event but also in its aftermath. The importance of charring characteristics in structural engineering lies in their positive impact on safe and reliable fire performance design. Accurate data on charring behavior allows for the development of more resilient timber structures and enhances the predictability of performance under fire scenarios. In fact, many research works on timber structures under fire conditions have been undertaken by the researchers previously. Fire performance of timber structural elements was investigated in most of the research on components such as beam elements, columns, connections, panels and slabs. The timber structures include wall panels, floors, and roofs, laminated timber beams or columns, laminated veneer lumber (LVL) beams , which generally maintain the load-bearing capacity by predictable charring, connection behaviour, and ventilation (Mitchelle et al., 2025). A research study by Vairo et al. (2023) analyzed the fire performance of cross-laminated timber (CLT)panels during and after a fire. It was observed that the CLT panels exhibit predictable charring behavior under standard ISO fire, with a linear charring rate of 0.6 mm/min–0.7 mm/min and char depth of 18 mm to 22 mm after 30 minutes. This predictable charring rate allows for reliable estimation of residual load-bearing capacity in fire design of CLT elements in buildings. Alrahman et al. (2025) found that the charring performance of the proposed wood-steel slab element was between 0.88 mm/min and 1.00 mm/min after exposure to fire. In the study conducted by Suzuki et al. (2016), the charring characteristics and failure modes of the structural elements under standard fire exposure were investigated. It was observed that the estimated charring rate of a Japanese cedar CLT panel was 0.78 mm/min to 0.66 mm/min, while the charring rate of LVL panels was approximately 0.6 mm/min, respectively. The performance of timber connections exposed to fire was reviewed by Maraveas et al. (2015). The fire performance of typical components of timber structure buildings has been documented (Wei et al.,2022).

The rate at which wood chars is influenced by a variety of factors, which have been consistently highlighted in the literature over several decades (Schaffer, 1967; White & Dietenberger, 2001; Njankouo et al., 2004; Yang et al., 2009). Among these factors, wood density is widely recognized as one of the most significant ones. Numerous studies have confirmed that denser timber species exhibit slower charring rates. For example, Dahunsi et al. (2015) demonstrated that high-density woods char at a markedly slower rate than lower-density counterparts, owing to their compact cellular structures and thermal mass. Wood density, however, is not uniform, it can vary significantly among species, within individual trees, and even across different parts of a single cross-section. At temperatures above 300°C where pyrolysis accelerates and wood transitions to char, the material's density may be reduced to approximately 20% of its original value. Schaffer (1967) was among the first to systematically study how timber species and density affect charring behavior under typical fire conditions, concluding that denser timbers significantly delay the onset and progression of charring. White and Dietenberger (2001) corroborated these findings, particularly noting that the effect of density is more pronounced in hardwoods than in softwoods. In addition to density, timber species plays a critical role in charring behavior due to differences in lignin, hemicellulose, and cellulose within the wood structure, chemical composition, and cell morphology, which influence degradation mechanisms under fire exposure (Parker, 1992; Kim et al., 2006).

National and international design codes, such as MS 544-Part 9 (2001) in Malaysia, and Eurocode 5 (EC5, 2004) and BS 5268 (1990) internationally, provide guidance on fire performance based on strength groups/classes or timber densities. In Malaysia, timber classification relies primarily on strength groups rather than an ascending or descending order of density. As a result, variations in fire performance must be carefully considered, particularly since Malaysian-grown species may behave differently from species of other countries due to climate-driven differences in growth conditions and wood properties.

Given the current research gaps, this study investigates the charring performance of solid Malaysian tropical hardwood by comparing two species with significantly different densities. The objective was to enhance understanding of how density influences charring behavior, thereby informing safer and more effective fire-resistant design practices for timber structures in Malaysia.

Materials and Methods

Preparation of timber materials

Malaysian tropical timbers, Resak (*Cotylelobium* sp.) and Jelutong (*Dyera costulata* sp.), with dimensions of 100 × 300 × 1400 mm (thickness × width × length), were sourced from a sawmill in Terengganu, Malaysia, and used as test specimens in this study. The timber samples were visually graded in accordance with the Malaysian Standard MS 1714:2003. Specification details on timber species, strength group, density, dimensions, number of specimens, and exposure durations are given in Table 1.

Table 1 Specification details of timber

Timber Species	Strength Group (SG)	Density (kg/m^3)	Dimensions	Exposure Durations (minutes)	Number of Specimen
Resak	SG4	1019	100x300x1400	60	3
Jelutong	SG6	506	100x300x1400	60	3

Preparation of the test setup

The furnace employed in this study had internal dimensions of 1500 mm × 1500 mm × 1500 mm and was powered by three liquefied petroleum gas (LPG) injection burners. It was equipped with three built-in thermocouples to monitor temperature distribution at various positions and heights within the chamber, as illustrated in Figure 2. The furnace interior was lined with a ceramic fiber-based heat-resistant fire blanket to minimize the diffusion of smoke and flames during testing. A vertically oriented front cover facilitated specimen placement and operator access. This cover, measuring at 130 mm × 1500 mm, was designed with three dedicated openings for the secure positioning of test specimens, as shown in Figure 3. To ensure containment and maintain safety, rock wool insulation functioning as a heat-resistant sealing material was used to tightly enclose each specimen within its slot, effectively preventing fire propagation beyond the furnace chamber. This setup ensured adequate thermal insulation and contributed to maintaining a stable and controlled fire testing environment. Furnace temperatures were continuously monitored by an experienced operator from the control room to ensure close adherence to the standard time–temperature curve defined in BS 476-20 (1987), as presented in Figure 4.

DOI: 10.5614/j.eng.technol.sci.2026.58.4.8

Figure 2 Interior view of the furnace.

Figure 3 Furnace cover with slotted speciment placement.

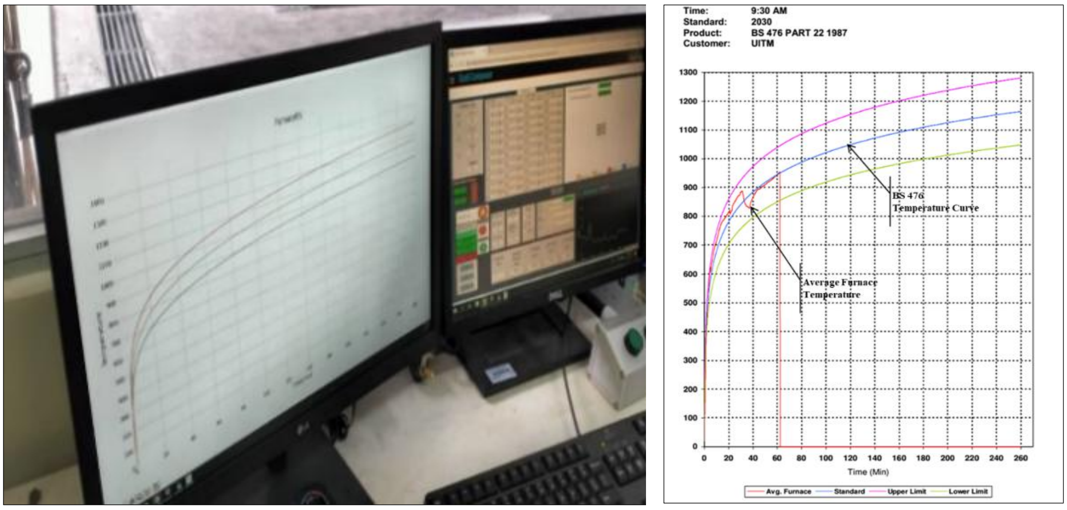

Figure 4 Standard temperature curve in Accordance with BS 467: Part 20.

To measure temperature progression during the fire test, six Type K thermocouples (diameter: 4.8 mm) were embedded vertically at six predetermined depths (6 mm, 12 mm, 18 mm, 24 mm, 30 mm, and 36 mm) within each timber specimen measured from exposed surface, with the 300 °C isotherm used as the critical reference point for charring analysis (Ilgın et al., 2023; Johansson & Svenningsson, 2018). The placement configuration is illustrated in the schematic diagram shown in Figure 5 where a series of holes were drilled vertically from the top surface of each specimen to accommodate these six thermocouples. Thermocouples were also positioned at 6 mm horizontal intervals across the cross-section, following a setup similar to that employed by König (2005). These sensors are rated for temperatures up to 1200 °C, making them suitable for high-temperature fire resistance testing.

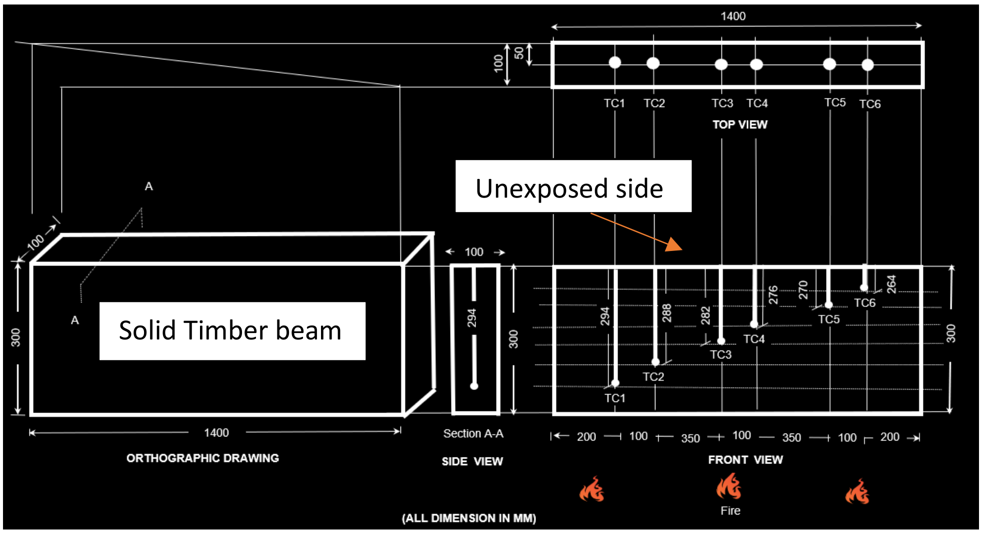

Figure 5 Schematic diagram for the position of thermocouples in the beam (in mm Units).

All thermocouples were connected to an electronic data acquisition system, which enabled continuous, real-time recording of temperature data throughout the duration of the fire exposure. After insertion, the specimens were mounted into the designated slots of the furnace's front cover. The thermocouples were oriented away from the direct furnace exposure, with specimens arranged to face three principal directions, bottom, top, and front representing varied fire exposure scenarios, as depicted in Figure 6. The bottom and top orientations simulated fire impact on horizontal structural members such as beams and roof trusses, whereas the front-facing setup represented fire exposure on vertical elements like walls or columns.

The fire test was conducted for a duration of 60 minutes, or until the designated target temperature was achieved, in accordance with standard fire testing protocols. Upon completion, the furnace was shut down, and the specimens were left to cool for about two minutes within the chamber to avoid thermal shock. Once partially cooled, they were carefully removed and transferred to a dry area, where they were lightly sprayed with water to suppress any ongoing combustion (Figure 7). This procedure was essential to prevent post-test charring and preserve the integrity of the charred layers. Subsequently, all specimens were prepared for post-fire examination, specifically for measuring the char depth to enable a comprehensive assessment of fire-induced material degradation. The charred specimens were cut to measure the char depth, as illustrated in Figure 8. Since six thermocouples were inserted into each sample, the specimen was divided into six sections, with each slice being approximately 10 mm thick (Figure 9).

Figure 6 Fire testing furnace with specimen ready for testing.

DOI: 10.5614/j.eng.technol.sci.2026.58.4.8

(a) (b)

Figure 7 After fire test ;(a) frame was removed from furnace and ; (b) samples were sprayed with water.

(a) (b) (c)

Figure 8 Preparation of charred samples; (a) charred beam before scrapping, (b) removing the char on the sliced specimen and (c) comparison between charred cross-section and original cross-section.

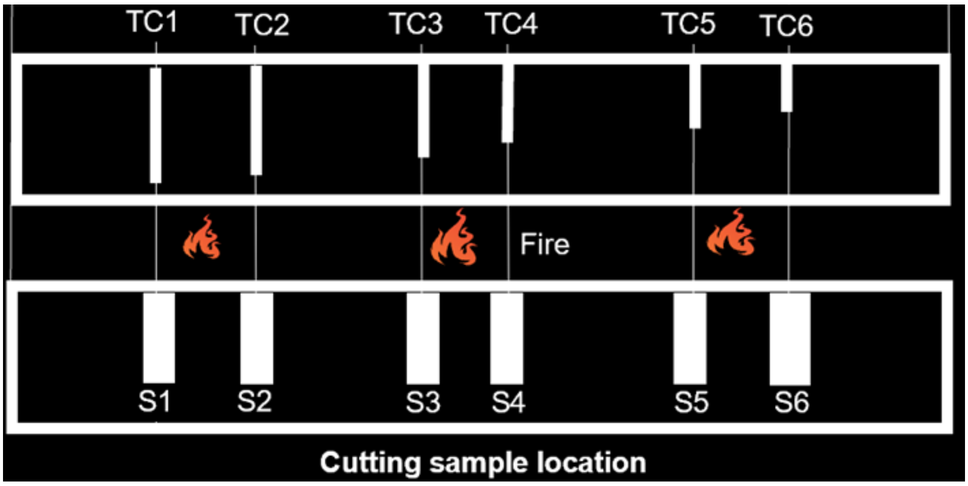

Figure 9 Schematic diagram for the cutting sample slice location at each of the thermocouples.

Determination of charring depth and charring rate

In this study, the charring depth and charring rate were determined based on direct and indirect measurement methods. For the direct method, the scrapped charred samples were photographed, and the detailed boundary lines were retraced using CAD software (Visio 2013). The area for determining char depth was divided into three parts as illustrated in Figure 10. To calculate the char depth, the thickness of the charred layer, d_{char}, was determined by averaging the depths from the two sections ($d_{char,1}$ and $d_{char,2}$) for each specimen. This average was then compared with the original cross-sectional thickness.

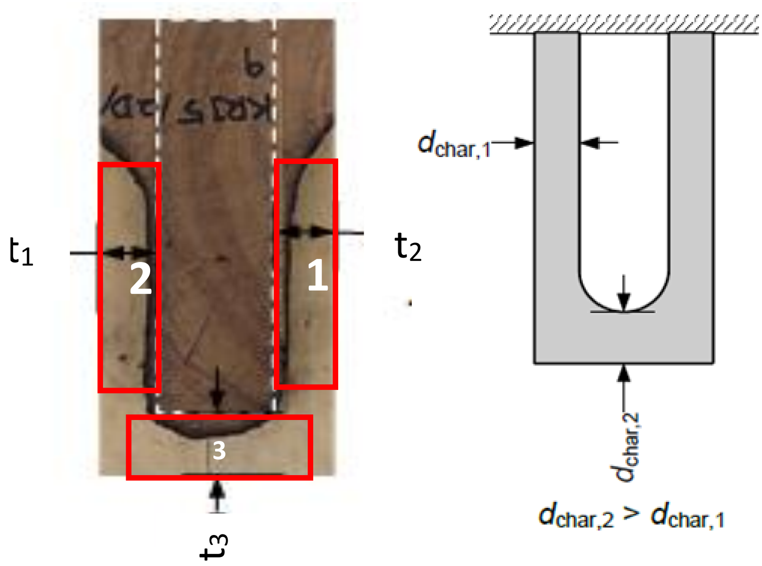

Figure 10 Preparation of determination of char depths: (a) Actual speciments (b) Method of measurement of char depth for three-sided fire exposure.

For the direct measurement of the residual cross-section, an average charring depth over the whole fire duration was then determined. The char depth calculation is as in Eqs. (1) and (2):

For Section 1 (wide side):

$$d_{char,1\,(avg)} = \frac{t_1+t_2}{2} \tag{1}$$

For Section 2 (narrow side):

$$d_{char,2} = t_3 \tag{2}$$

To calculate the charring rate for two-dimensional fire exposure, β_n , the charring depth were taken from an average $\beta_{char,1(avg)}$ and $\beta_{char,2}$. The predicted charring rate can be derived using the linear model provided in EN 1995-1-2, as expressed in Eq. (3):

$$\beta_n = \frac{d_{char}}{t} \tag{3}$$

Where; β_n represents the two-dimensional charring rate (mm/min); d_{char} as the charring depth for two-dimensional charring (mm); and t as time of fire exposure (minute).

Results

Visual observations

Figure 11 presents a series of visual observations captured during the two-dimensional fire test. Following the initial exposure to fire, visible flames were observed through the furnace's glass inspection window. As the internal temperature increased, the emergence of white smoke became apparent, with its intensity escalating significantly in tandem with the temperature rise (Figure 11a). Subsequently, a distinct char layer began to develop on the fire-exposed surface. This layer, indicative of the thermally degraded material, progressively thickened as pyrolysis advanced (Figure 11b). On the unexposed surface, visible signs of moisture evaporation were detected (Figure 11c), indicating that the timber had likely reached a surface temperature near 100 °C corresponding to the boiling point of water within the material. As heating continued, the external surface of the wood darkened, accompanied by the appearance of flames through cracks in the timber. Post-fire examination, as depicted in Figure 12, revealed a clearly distinguishable char layer characterized by its dark black coloration and porous texture, consistent with descriptions of charred wood in the literature (Pinto et al., 2016).

DOI: 10.5614/j.eng.technol.sci.2026.58.4.8

The fire-exposed timber exhibited three distinct zones (Figure 12): the char layer, the pyrolysis zone, and the unburnt core. These regions were visually identifiable, highlighting the progressive thermal degradation of the specimens under fire conditions. Following exposure to the standard fire curve, a noticeable reduction in cross-sectional area was observed. Additionally, corner regions exhibited a transformation from sharp rectangular profiles to more rounded edges, attributed to multidirectional heat exposure. This phenomenon of corner rounding, evident in both Figures 12 and 10a, is a characteristic of two-dimensional charring, which accounts for accelerated degradation at edges and corners as outlined in EN 1995-1-2 (2004). Notably, the two timber species demonstrated distinct charring behaviors. Resak exhibited fine, interconnected surface fissures resembling a “crocodile skin” or “map-like” cracking pattern (Figure 13a), while Jelutong developed larger, block-type cracks (Figure 13b).

(a) (b) (c)

Figure 11 Visual observation during fire test; (a) Flame and smoke build up inside the furnace and (b) formation of char for Resak and (c) evaporation of moisture due to heat.

Figure 12 Visual observation after fire test.

(a) (b)

Figure 13 Charring on the lateral surface of; (a) Resak and (b) Jelutong.

Charring depth and charring rate

Table 1 presents the measured charring depths on the lateral and bottom surfaces of Resak and Jelutong specimens after exposure to fire. For Resak, the average lateral charring depth ($d_{char,1\,(avg)}$) was slightly lower than the bottom charring depth ($d_{char,2}$), whereas Jelutong exhibited the opposite trend, with the lateral side showing greater char penetration than the bottom side. Visual inspection of the charred surfaces, particularly for Jelutong, revealed notable irregularities and uneven char profiles on the lateral faces. Based on direct measurements (Table 2), Resak exhibited the shallowest char penetration , while Jelutong showed the deepest after 60 minutes of fire exposure.

Table 2 Char depth and charring rate for Resak and Jelutong.

Species	Diagrams of cross-section	Specimen	Lateral sides $d_{char,1\,(avg)}$ (mm)	Bottom sides $d_{char,2}$ (mm)	Charring Rate β_n(mm/min)
		RSK-B1-TC1	26.5	29.0	
		RSK-B1-TC2	24.5	25.0	
		RSK-B1-TC3	24.0	24.0	
		RSK-B1-TC4	23.5	22.0	
		RSK-B1-TC5	26.0	26.0	
		RSK-B1-TC6	25.5	25.0	
		RSK-B2-TC1	24.0	28.0	
		RSK-B2-TC2	25.0	26.0	
		RSK-B2-TC3	26.0	26.0	
Resak	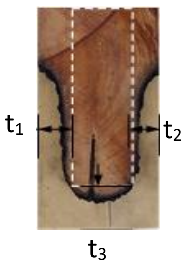	RSK-B2-TC4	27.5	27.0	0.48
		RSK-B2-TC5	26.0	28.0	
		RSK-B2-TC6	27.5	28.0	
		RSK-B3-TC1	16.5	16.0	
		RSK-B3-TC2	16.0	14.0	
		RSK-B3-TC3	17.5	16.0	
		RSK-B3-TC4	17.5	15.0	
		RSK-B3-TC5	9.0	18.0	
		RSK-B3-TC6	8.0	16.0	
		Average	21.7	54.0	
		JLG-B1-TC1	38.5	32.0	
		JLG-B1-TC2	35.5	29.0	
		JLG-B1-TC3	45.5	40.0	
		JLG-B1-TC4	46.5	42.0	
		JLG-B1-TC5	42.5	43.0	
		JLG-B1-TC6	47.0	39.0	
		JLG-B2-TC1	48.5	35.0	
		JLG-B2-TC2	46.5	35.0	
		JLG-B2-TC3	47.0	34.0	
Jelutong	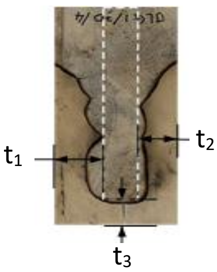	JLG-B2-TC4	49.5	34.0	0.83
		JLG-B2-TC5	48.5	33.0	
		JLG-B2-TC6	47.0	34.0	
		JLG-B3-TC1	41.0	32.0	
		JLG-B3-TC2	42.5	38.0	
		JLG-B3-TC3	39.0	34.0	
		JLG-B3-TC4	41.0	36.0	
		JLG-B3-TC5	42.5	38.0	
		JLG3-B3-TC6	42.0	34.0	
		Average	43.9	53.0	

Notes: RSK- Resak; JLG – Jelutong; TC1- Thermocouple No.1 for TC1; B1 - Beam no.1; t_1 and t_2 for lateral sides;t_3 for bottom sides

The progression of the charring front within the solid timber beams is illustrated in Figures 14 and 15 for Resak and Jelutong, respectively. These figures enable interpretation of the charring development over time and allow for the calculation of charring rates based on thermocouple measurements at various depths, as detailed in Figure 5. A reference temperature of 300 °C was adopted as the threshold for charring, and the time taken for each thermocouple to reach this temperature from the initiation of the fire test was recorded. In terms of material density, the lower-density Jelutong timber (density < 600 kg/m³) reached the 300 °C isotherm at approximately 25 minutes, whereas the higher-density Resak timber (density > 600 kg/m³) exhibited a delayed thermal response, reaching the same temperature approximately 30 minutes later.

DOI: 10.5614/j.eng.technol.sci.2026.58.4.8

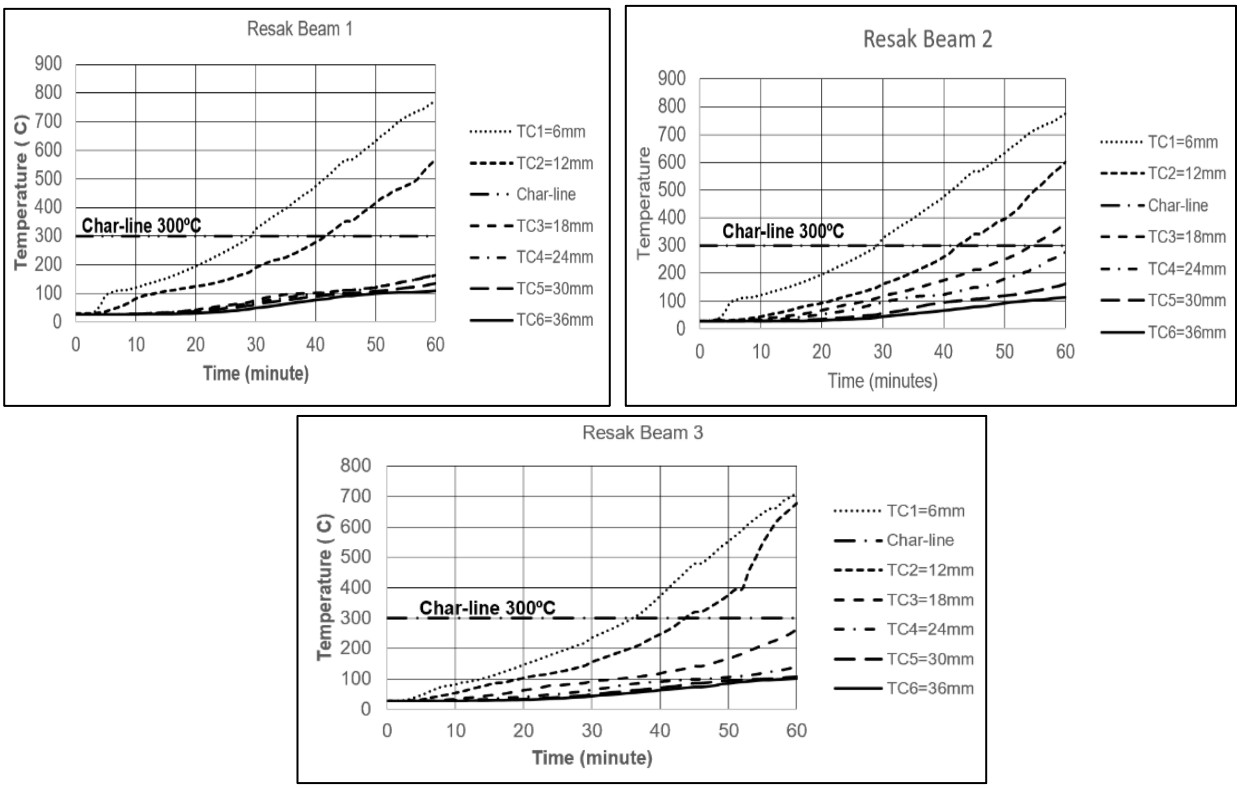

Figure 14 Temperature-Time relationships for Resak.

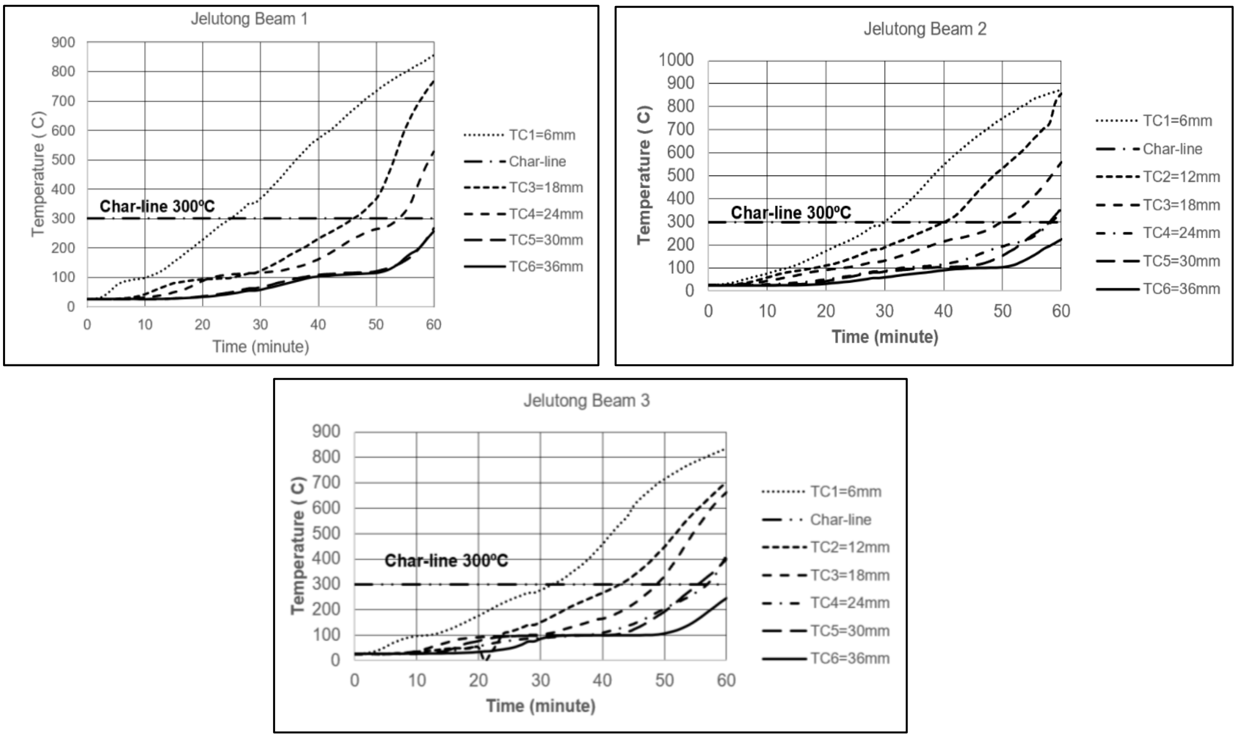

Figure 15 Temperature -Time relationships for Jelutong.

Figure 16 presents the measured charring depths for each Resak and Jelutong specimen. Both timber types exhibited comparable surface charring behavior; however, notable differences in maximum charring depth were observed. Resak, with a density of 1019 kg/m³, reached a maximum charring depth of 18.0 mm, whereas Jelutong, with a significantly lower density of 506 kg/m³, exhibited a greater charring depth of 30 mm.

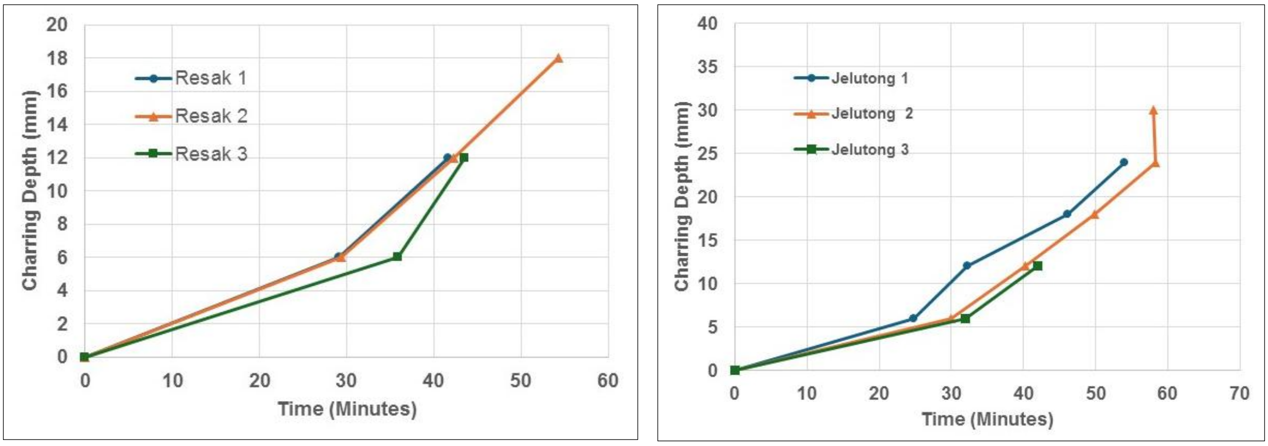

(a) (b)

Figure 16 Charring depth versus time for; (a) Resak and (b) Jelutong wood samples at 300°C reference temperature.

Discussion

The results of this study clearly demonstrate the sequential process of timber degradation under fire exposure, comprising moisture evaporation, pyrolysis, and char formation. The presence of a temperature plateau at approximately 100 °C demonstrates the energy absorbed during moisture evaporation, which delays temperature rise within the timber. As heating continued, the external surface of the wood darkened, accompanied by the appearance of flames through cracks in the timber. This phenomenon marked the onset of pyrolysis, a critical phase of thermal decomposition that typically begins between 260 °C and 300 °C (Frangi et al., 2009). During this phase, combustible volatiles were released, and significant timber mass loss occurred due to both moisture migration and evaporation (Tsantaridis, 2003). It was found that the differences in crack morphology are indicative of the material density, with Resak having a higher density showing finer crack patterns compared to the more coarsely cracked, lower-density Jelutong.

Both Resak and Jelutong exhibit similar thermal response patterns, characterized by a plateau near 100 °C in the temperature-time profiles. This plateau corresponds to the phase of moisture evaporation, as timber reaches the boiling point of water, initiating bound water release from the wood cell structure—an observation consistent with findings by Njankouo et al. (2004). During this stage, significant thermal energy is diverted from heating the timber to facilitate phase change, thereby slowing the rate of temperature increase. The energy requirement increases with the volume of moisture to be evaporated and is further influenced by heat losses through convective transfer (Di Blasi et al., 2017). Experimental observations reveal that this plateau phase extends in duration with increasing distance from the fire-exposed surface. This reflects the time required for heat to conduct through the timber mass and the moisture gradient present. Until the majority of moisture is expelled, the temperature remains relatively constant, which in turn affects the thermal properties of the wood—such as conductivity and specific heat—alongside ignition delay and combustion rates (Spearpoint & Quintiere, 2000). Once the timber is sufficiently dried, a rapid rise in temperature is observed, indicating a shift in thermal behavior. Shen et al. (2007) noted that higher moisture content suppresses surface temperatures and reduces charring rates. This moisture-driven retardation, commonly referred to as the "cooling phase," increases the heat demand and may contribute to higher structural vulnerability if prolonged (Horne et al., 2023). Beyond the 300 °C threshold, the material transitions into a charred state, forming a low conductivity insulating layer. This char layer introduces a steep thermal gradient and serves as a protective barrier, limiting heat penetration into the unburned timber core.

The char penetration results clearly demonstrate that timber density significantly influences charring behaviour. Higher-density timber (Resak) demonstrated greater resistance to charring compared to lower-density timber (Jelutong). These findings are aligned with the results reported by Gardner and Syme (1991), who observed a similar density-dependent relationship in a comparative two-hour study of eight hardwood and softwood species. The results reinforce the understanding that wood density is a key parameter affecting charring resistance and must be considered in fire design for timber structures. The results are also consistent with the guidance provided in EN 1995-1-2, which estimates

DOI: 10.5614/j.eng.technol.sci.2026.58.4.8

charring depths of approximately 40 mm for general structural timbers and around 30 mm for denser hardwoods (with nominal densities ≥650 kg/m³ at 18% moisture content) after one hour of fire exposure. The observed performance of Resak, with a density exceeding 650 kg/m³, supports its classification as a hardwood with enhanced fire resistance, given its significantly lower charring depth compared to the standard prediction.

Furthermore, the progression of the charring front within the solid timber beams highlights that an increase in wood density corresponds to a slower rate of temperature rise within the timber section, as higher-density specimens require more time to approach the ambient furnace temperature. This trend is aligned with the findings reported by Zhang et al. (2012), which similarly demonstrated that denser timbers exhibit greater resistance to thermal penetration.

The results further validate the inverse relationship between wood density and charring rate, with Resak having a higher density (1019 kg/m³), exhibited a slower charring rate of 0.48 mm/min, while Jelutong, a lower-density species (506 kg/m³), showed a noticeably faster charring rate of 0.83 mm/min. This trend aligns with previous studies demonstrating that denser timbers generally char more slowly due to their compact cellular structure, lower porosity, and greater thermal inertia. This outcome supports the well-established understanding that both timber species and wood density significantly influence charring behavior, as echoed in previous studies (Wang et al., 2025; Liu & Fischer, 2024; Li et al., 2023; Barlett et al., 2019; Friquin 22011;König 2005; Njankouo et al., (2004). Wang et al., (2025) found that Larch timber with high density (563 kg/m³) had slower rate compared to lower density Douglas fir (498 kg/m³) and China fir (379kg/m³). Similar findings were reported by Liu & Fischer (2024) and Barlett et al.,(2019) reported that hardwoods with densities above 700 kg/m³ exhibit charring rates below 0.6 mm/min, while timbers with lower densities, had higher rates with more than 0.8 mm/min. The authors observed that high-density hardwoods form a more stable and insulating char layer that reduces heat penetration. Li et al., (2023) also noted that hardwoods with densities above 900 kg/m³ tend to develop a more uniform and protective char layer with fewer cracks, further limiting heat penetration from the surface to the inner core of the timber. Similarly, investigations by Friquin (2011) and König (2005) highlighted that the charring rate decreases almost linearly with increasing oven-dry density, emphasizing the important role of density in heat transfer resistance. Njankouo et al., (2004) also found that wood density has a significant impact on the charring rate. A decrease in the charring rate was noted for tropical hardwood species with densities greater than 500kg/m³.

The current design standards and codes including EC5 (2004), MS544 (2001), AS/NZS 1720.4 (2019), and ANSI/NDS SUPP (2018) which provide recommended charring rates based on timber classification, such as species type, density, and strength grouping. Specifically, Malaysian Standard MS544 recommends a charring rate of 0.5 mm/min for timbers in higher strength groups and 0.7 mm/min for lower strength classes. The experimental findings indicate that both Resak and Jelutong charred at rates slightly below those prescribed by MS544. When compared to the 0.55 mm/min rate for hardwoods specified in Eurocode 5 (EC5, 2004), both species were found to be in close alignment with this European benchmark. These results clearly underscore the critical role of timber selection in influencing charring performance, reinforcing the necessity for species-specific assessments in fire design.

Conclusion

This study highlights the distinct charring behavior of two Malaysian tropical timber species namely Resak and Jelutong under standardized fire exposure. The results revealed clear differences in fire performance driven primarily by timber density and species characteristics. For Resak, a denser hardwood, the average charring depth on the lateral sides was slightly lower than on the bottom face. In contrast, Jelutong, a lower-density timber, exhibited greater charring on the lateral surfaces compared to the bottom. The average charring rates were found to be 0.48 mm/min for Resak and 0.83 mm/min for Jelutong, both of which fall within the range prescribed by Eurocode 5 for hardwood species. The measured charring rates support a better prediction of how much structural capacity remains during a fire. The alignment of the results with Eurocode 5 benchmarks also reinforces their suitability for incorporation into Malaysian Standard MS544, particularly fire resistance for local tropical timbers. This strengthens confidence in using Malaysian timber for construction. By supplying empirical data for Malaysian timber species, this study strengthens the technical basis for updating national design standards, improving fire performance prediction, and guiding engineers and architects in selecting appropriate timber materials for compliant and fire-safe construction. These findings reaffirm the established correlation between wood density and charring behavior. Denser timbers such as Resak not only char more slowly but also offer improved fire resistance, making them more suitable for structural applications where fire safety is a critical design consideration. Jelutong's higher charring rate reflects its lower density and reduced resistance to thermal degradation, underscoring the importance of timber selection in fire engineering design.

The study also highlights the limitations of applying uniform charring rates without considering species-specific properties, which may lead to either overly conservative or unsafe fire design. Consequently, further research is recommended to expand the database of fire performance characteristics for a broader range of Malaysian tropical hardwoods and softwoods. Additionally, future research should focus on examining the influence of density, grain orientation, moisture content, and anatomical structure on thermal degradation will enhance the accuracy and applicability of national and international fire design standards. A more comprehensive understanding of local timber behavior under fire conditions will ultimately contribute to safer, more efficient timber structure designs in tropical climates.

Acknowledgement

The authors would like to acknowledge the Fire Protection Laboratory at the Forest Research Institute Malaysia (FRIM), the Research Management Centre at Universiti Teknologi MARA (UiTM), and the Faculty of Civil Engineering, UiTM, for their invaluable laboratory and administrative support.

Compliance with ethics guidelines

The authors declare they have no conflict of interest or financial conflicts to disclose.

This article contains no studies with human or animal subjects performed by the authors.

References

Australian/New Zealand Standard (AS/NZS), (2019). Timber Structures Part 4: Fire Resistance of Timber Elements, AS/NZS 1720.4:2019, Standard Australia Limited/ Standards New Zealand.

BS 476-20 (1987). Fire tests on building materials and structures. Method for determination of the fire resistance of elements of construction. BSI British Standard.

Cachim, P. B., & Franssen, J. M. (2009). Comparison between the charring rate model and the conductive model of Eurocode 5. *Fire and Materials: An International Journal*, *33*(3), 129–143. https://doi.org/10.1002/fam.985

Dahunsi, B.I.O., Adetayo, O.A. (2015). Burning characteristics of some selected structural timber species of Southwestern Nigeria. *IOSR Journal of Mechanical and Civil Engineering*, *12*(4),112–120.

Di Blasi, C., Branca, C., & Galgano, A. (2017). On the experimental evidence of exothermicity in wood and biomass pyrolysis. *Energy Technology*, *5*(1), 19–29. https://doi.org/10.1002/ente.201600091

EN 1995-1-2: (2004). Eurocode 5: Design of Timber Structures—Part 1–2: General—Structural Fire Design. European Committee for Standardization: Brussel, Belgium, 2004.

EN13381-7. (2019). Test methods for determining the contribution to the fire resistance of structural members. *BSI British Standard.*

Frangi, A., Fontana, M., Hugi, E., Jübstl, R., & Robert, J. (2009). Experimental analysis of cross-laminated timber panels in fire. *Fire Safety Journal*, *44*(8), 1078–1087. https://doi.org/10.1016/j.firesaf.2009.07.007

Friquin K.L. (2011). Material properties and external factors influencing the charring rate of solid wood and glue-laminated timber. *Fire Material, 35*, 303–327. https://doi.org/ 10.1002/fam.1055.

Gardner W.D. & Syme D.R. (1991). Charring of Glue-Laminated Australian-Grown Timber Species and the Effect of 13 mm Gypsum Plaster-Board on Their Charring. Technical Report No. 5, NSW Timber Advisory Council Ltd., Sydney, Australia.

Horne, P., Abu, A., Palermo, A. & Moss, P. (2023). Thermal response of timber connections in the cooling phase. *Fire and Materials*, *47*(4), pp.479–497. https://doi.org/10.1002/fam.3136

Ilgın, Hüseyin Emre, Markku Karjalainen, Mika Alanen, and Mikko Malaska. (2023). Evaluating fire performance: An experimental comparison of dovetail massive wooden board elements and cross-laminated timber. *Fire, 6*(9),352. https://doi.org/10.3390/fire6090352.

Johansson, E. & Svenningsson, A.(2018). Delamination of cross-laminated timber and its impact on fire development. Focusing on different types of adhesives; Report 5562; Division of Fire Safety Engineering, Lund University: Lund, Sweden.

Kim, H. S., Kim, S., Kim, H. J., & Yang, H. S. (2006). Thermal properties of bio-flour-filled polyolefin composites with different compatibilizing agent type and content. *Thermochimica acta*, *451*(1-2), 181–188. https://doi.org/10.1016/j.tca.2006.09.013

König, J. (2005). Structural fire design according to Eurocode 5—design rules and their background. *Fire and Materials*, *29*(3), 147–163. https://doi.org/10.1002/fam.873.

Li X, Zhang X, Hadjisophocleous G, & McGregor C. (2015). Experimental study of combustible and non-combustible construction in a natural fire. *Fire Technol*, *51*(6),1447–74. https://doi.org/10.1007/s10694-014-0407-4.

Liu, J. & Fischer, E.C. (2024). Review of the charring rates of different timber species. *Fire and Materials*, *48*(1), pp.3–15. https://doi.org/10.1002/fam.3173.

DOI: 10.5614/j.eng.technol.sci.2026.58.4.8

MS 1714. (2003). Specification for visual strength grading of tropical hardwood timber. SIRIM Bhd., Malaysia.

MS 544 Part 2. (2001). Code of Practice for Structural Use of Timber. Department of Standard, Malaysia. Department of Standard, Malaysia.

MS 544 PART 9. (2001). MS 544: PART 9 : SECTION 1 : 2001 Code of Practice for Structural Use of Timber : Part 9 : Fire Resistance of Timber Structures : Section 1 : Method of Calculating Fire Resistance of Timber Members.

National Design Specification (NDS) for Wood Construction (2018). ANS/NDS SUPP-2018, Fire Design of Wood Members, American Wood Council.

Njankouo, J. M., Dotreppe, J. C., & Franssen, J. M. (2004). Experimental study of the charring rate of tropical hardwoods. *Fire and materials*, *28*(1), 15–24. https://doi.org/10.1002/fam.831.

Parker W.J .(1992). Heat release in fires. In: Babrauskas V, Grayson SJ (eds) Wood Materials – prediction of the heat release from basic measurements. Elsevier Applied Sciences, New York.

Peng, Lei, George Hadjisophocleous, James R. Mehaffey & Mohammad Mohammad .(2010). Fire resistance performance of unprotected wood–wood–wood and wood–steel–wood connections: A literature review and new data correlations. *Fire Safety Journal, 45*, 392–399. https://doi.org/10.1016/j.firesaf.2010.08.003.

Pinto, E. M., Machado, G. D. O., Felipetto, R. P. F., Christoforo, A. L., Lahr, F. A. R., & Calil Jr, C. (2016). Thermal degradation and charring rate of and wood species. *The Open Construction & Building Technology Journal*, *10*(1). https://doi.org/10.2174/1874836801610010450.

Richter F, & Rein G. (2019). Heterogeneous kinetics of timber charring at the microscale. *J Anal Appl Pyrolysis, 138*, 1–9. https://doi.org/10.1016/j.jaap.2018.11.019.

Richter, F., Kotsovinos, P., Rackauskaite, E., & Rein, G. (2021). Thermal response of timber slabs exposed to travelling fires and traditional design fires. *Fire Technology*, *57*, 393–414. https://doi.org/10.1007/s10694-020-01000-1.

Schaffer, E. L. (1967). Review of information related to the charring rate of wood (Vol. 145). Forest Products Laboratory.

Shen, D. K., Fang, M. X., Luo, M., Cen, K. F., & Chow, W. K. (2007). Thermal degradation and ignition of wood by thermal radiation. *Fire Safety Sci, 7*, 90–102.

Spearpoint, M. J., & Quintiere, J. G. (2000). Predicting the burning of wood using an integral model. *Combustion and flame, 123*(3), 308–325. https://doi.org/10.1016/S0010-2180(00)00162-0.

Syme D. (1994). Verification of charring equations for Australian timbers based on full-scale fire resistance tests. In: Conference proceedings—Pacific timber engineering conference, vol. 1. Australia: Queensland University of Technology. pp. 619–623.

Tsantaridis, L. (2003).Reaction to fire performance of wood and other building products. Ph.D. Thesis, Kungliga Tekniska Högskolan, Stockholm, Sweden, 2003.

White R. H. & Dietenberger M. A. (2001). Wood products: Thermal degradation and fire. *Encycl. Mater. Sci. Technol*., pp. 9712–9716. https://doi.org/10.1016/B978-0-12-803581-8.03338-5.

Yang, T H, Wang, S Y, Tsai, M J & Lin, C Y. (2009). The charring depth and charring rate of glued laminated timber after a standard fire exposure test. *Building and Environment*, *44*(2), 231–236. https://doi.org/10.1016/j.buildenv.2008.02.010.

Zhang, J.; Xu, Q.-F.; Xu, Y.-X.; Wang, B.; & Shang, J.-X. (2012). A numerical study on fire endurance of wood beams exposed to three-sided fire. *J. Zhejiang Univ*. *Sci.* A, *13*, 491–505. https://doi.org/10.1631/jzus.A1200022.

Manuscript Received: 9 July 2025
Revised Manuscript Received: 21 November 2025
Accepted Manuscript: 6 May 2026